EUROPEAN ORGANIZATION FOR NUCLEAR RESEARCH

L3 Note 2770
July 19^{th} 2002

Production of Z Boson Pairs at LEP

The L3 Collaboration

Abstract

We present results on the pair production of Z bosons in the data collected by the L3 detector in e^+e^- collisions at center–of–mass energies from 183 GeV up to 209 GeV at LEP. The cross section of this process is measured, and the results are found to be in agreement with the Standard Model predictions. Limits on triple couplings between neutral gauge bosons, forbidden in the Standard Model, are derived from these measurements. Results for center–of–mass energies above 204 GeV are preliminary.

Submitted to the *XXXIst International Conference on High Energy Physics*
July 24 - July 31, 2002, Amsterdam, Netherlands.

1 Introduction

The threshold energy for Z-Pair production has been passed by the LEP collider in the year 1997. Since then, over 680 pb^{-1} of data have been accumulated by the L3 experiment, thus allowing to study this process. Besides of its understanding as an irreducible background for the search of the Standard Model Higgs Boson and for other possible theories beyond the Standard Model, it allows the study of triple neutral gauge boson couplings, ZZZ and ZZγ [1], forbidden at tree level in the Standard Model.

The experimental investigation of Z pair production is made difficult by its rather low cross section, compared with competing processes that constitute large and sometimes irreducible backgrounds. The existence at threshold of this process was established at $\sqrt{s} = 183$ GeV [2] and studies with higher statistics were presented with the data collected at 189 GeV [3] and at 192 – 202 GeV [4]. Results from other experiments were also reported in references [5–7]. In this note, the measurement of the cross section for center–of–mass energies up to 209 GeV is presented and a study on possible anomalous couplings among neutral gauge bosons is performed.

2 Data and Monte Carlo Samples

The investigated data were collected in the year 2000 by the L3 detector [8] at center–of–mass energies between 200 GeV and 209 GeV, and amount to a total integrated luminosity of $217.3\,\mathrm{pb}^{-1}$. These data are grouped into two subsamples. The breakdown into integrated luminosities and center–of–mass energies reads: $78.5\,\mathrm{pb}^{-1}$ at 204.8 GeV and $138.9\,\mathrm{pb}^{-1}$ at 206.6 GeV.

The EXCALIBUR [9] Monte Carlo is used to generate events belonging to both the signal and the background neutral–current four–fermion processes. Background from fermion–pair production is described making use of the KK2f [10] ($\mathrm{e^+e^-} \rightarrow \mathrm{q\bar{q}}(\gamma)$), KORALZ 4.02 [11] ($\mathrm{e^+e^-} \rightarrow \mu^+\mu^-(\gamma)$ and $\mathrm{e^+e^-} \rightarrow \tau^+\tau^-(\gamma)$) and BHWIDE [12] ($\mathrm{e^+e^-} \rightarrow \mathrm{e^+e^-}(\gamma)$) Monte Carlo generator programs. Background from charged–current four–fermion processes is generated with EXCALIBUR for the $\mathrm{e}\nu_\mathrm{e}\mathrm{q\bar{q}'}$ and $\ell^+\nu_\ell\ell^-\bar{\nu}_\ell$ ($\ell = \mathrm{e}, \mu, \tau$) final states and KORALW 1.21 [13] for other W-pair mediated processes. Contributions from multiperipheral processes are modelled by PHOJET 1.05c [14] ($\mathrm{e^+e^-} \rightarrow \mathrm{e^+e^-q\bar{q}}$) and DIAG36 [15] ($\mathrm{e^+e^-} \rightarrow \mathrm{e^+e^-}\ell^+\ell^-$).

The L3 detector response is simulated using the GEANT 3.15 program [16], which takes into account the effects of energy loss, multiple scattering and showering in the detector. Time dependent detector inefficiencies, as measured in the data taking period, are reproduced in these simulations.

The definition of the Z pair signal proceeds through kinematic requirements to the four final state fermions [2–4]: the invariant mass of both generated fermion-antifermion pairs must be between 70 GeV and 105 GeV. This criterion has to be satisfied by at least one of the two possible pairings of four same flavour fermions. In five cases the fermion pairs can originate from a charged–current process ($\mathrm{u\bar{u}d\bar{d}}$, $\mathrm{c\bar{c}s\bar{s}}$ and $\nu_\ell\bar{\nu}_\ell\ell^+\ell^-$, with $\ell = \mathrm{e}, \mu, \tau$). The invariant masses of the fermion pairs which could come from W decays are required to be either below 75 GeV or above 85 GeV. Events with electrons in the final state are rejected if $|\cos\theta_\mathrm{e}| > 0.95$, where θ_e is the electron polar angle. The last requirement reflects the L3 central tracker angular coverage and helps in rejecting multiperipheral contribution to the signal definition. The cross sections for the two considered center–of–mass energy points of 204.8 GeV and 206.6 GeV are 1.07 pb and 1.08 pb, respectively.

3 Event Selection

All visible final states of the Z pair decay are investigated, with criteria similar to those at $\sqrt{s} = 192 - 202$ GeV [4], with the exception of the $\mathrm{q\bar{q}q'\bar{q}'}$ channel for which a new analysis is devised. This analysis will be described in what follows.

After a high-multiplicity preselection that requires well-balanced hadronic events with large visible and small missing energy, remaining events are forced into four jets, and a kinematic fit imposing four-momentum conservation is performed to improve the di-jet mass resolution.

For the three possible jet pairings a discriminating χ^2_{ZZ} variable is built, and the pairing which minimizes

$$\chi^2_{ZZ} = \left(\Sigma_i - 2m_z\right)^2 / \sigma^2_{\Sigma_{ZZ}} + \Delta_i^2 / \sigma^2_{\Delta_{ZZ}}$$

is chosen, i denoting the pairing, Σ_i and Δ_i the dijet mass sum and difference, and $\sigma^2_{\Sigma_{ZZ}}$ and $\sigma^2_{\Delta_{ZZ}}$ their resolution. Events where the sum of the two dijet masses of this pairing exceeds 165 GeV are considered further. Then, ten discriminating variables x_i are combined into a discriminant using a likelihood technique:

$$\mathrm{L_{ZZ}} = \frac{\prod_\mathrm{i} \mathrm{p^i_{ZZ}}}{\sum_\mathrm{j} \prod_\mathrm{i} \mathrm{p^i_j}}, \qquad \mathrm{p^i_j} = \frac{\mathrm{f^j(x_i)}}{\sum_\mathrm{k} \mathrm{f^k(x_i)}},$$

where i denotes the *i-th* variable, and j and k the event class (ZZ signal, background, ...). Only events where $\mathrm{L_{ZZ}}$ exceeds a threshold that is optimized to maximize the sensitivity to the ZZ signal are selected.

The yields of all selections are summarised in Table 1, where the event numbers and efficiencies for both center–of–mass energy points have been summed up.

Selection	Data	Signal MC	Background MC	Efficiency
$\mathrm{q\bar{q}q'\bar{q}'}$	466	71.5	395.6	64%
$\mathrm{q\bar{q}}\nu\bar{\nu}$	49	19.6	29.3	30%
$\mathrm{q\bar{q}}\ell^+\ell^-$	28	19.1	4.6	55%
$\ell^+\ell^-\nu\bar{\nu}$	5	2.4	1.9	26%
$\ell^+\ell^-\ell'^+\ell'^-$	1	1.1	0.7	34%

Table 1: Data, signal and background Monte Carlo events selected by each analysis with their correpsonding efficiency. The numbers include all the center–of–mass energies. The $\mathrm{q\bar{q}}\nu\bar{\nu}$ entry is reported for a benchmark selection requirement of 0.5 on the neural network output.

For each of the selections, the most significant variable to distinguish between signal and background is chosen. For the $\mathrm{e^+e^-} \rightarrow \mathrm{ZZ} \rightarrow \mathrm{q\bar{q}q'\bar{q}'}$ final states, this variable is a combination of the logarithm of the selection likelihood, $\log \mathrm{L_{ZZ}}$, the sum of the two reconstructed Z masses, the logarithm of the jet resolution parameter $\log \mathrm{Y_{34}^{JADE}}$, and the event thrust. This distribution is displayed in figure 1a. For the $\mathrm{e^+e^-} \rightarrow \mathrm{ZZ} \rightarrow \mathrm{q\bar{q}}\nu\bar{\nu}$ analysis the neural network output variable shows the best separation between signal and background. It is shown in figure 1b. For the $\mathrm{e^+e^-} \rightarrow \mathrm{ZZ} \rightarrow \mathrm{q\bar{q}}\ell^+\ell^-$ final states the most significant variable is the output of a constrained kinematic fit that requires energy and momentum conservation and additionally the hadronic and leptonic systems to have the same invariant masses within their resolutions. Electrons, muons and taus are considered. This variable, M_{5C} is presented in Figure 1c. For the $\mathrm{e^+e^-} \rightarrow \mathrm{ZZ} \rightarrow \ell^+\ell^-\nu\bar{\nu}$ and $\mathrm{e^+e^-} \rightarrow \mathrm{ZZ} \rightarrow \ell^+\ell^-\ell'^+\ell'^-$ final states, the final variable is the sum of the invariant and recoil masses of a pair of electrons or muons consistent with a Z boson decay. The distribution of this variable for both states is shown in figure 1d.

4 Measurement of the ZZ Cross Section

The ZZ cross-section $\sigma_{\rm ZZ}$ is determined by a binned log-likelihood fit to the distributions of the most discriminating variables described above. By assuming the Standard Model predictions for the relative weights of all visible channels, the ZZ cross section $\sigma_{\rm ZZ}$ for the two investigated center–of–mass energies is found to be:

$$\sigma_{\rm ZZ}(204.8~{\rm GeV}) = 0.89^{+0.24}_{-0.21} \pm 0.07\,{\rm pb}~~({\rm SM} : 1.07\,{\rm pb})$$

$$\sigma_{\rm ZZ}(206.6~{\rm GeV}) = 1.24^{+0.20}_{-0.19} \pm 0.09\,{\rm pb}~~({\rm SM} : 1.08\,{\rm pb})$$

in good agreement with the expected cross sections within the signal definition cuts, reported in parentheses. The first quoted uncertainty is statistical while the second is systematic [4]. In figure 2, these data are presented together with previously published cross–section measurements and the evolution of the ZZ cross-section as a function of $\sqrt{s}$ as predicted by the Standard Model. The above results can also be interpreted in terms of the NC02 ansatz, the production of the four fermions through the t and u channel diagrams with two Z bosons. The NC02 cross sections extracted from the previous results are:

$$\sigma^{\rm NC02}_{\rm ZZ}(204.8~{\rm GeV}) = 0.88^{+0.24}_{-0.21} \pm 0.07\,{\rm pb}~~({\rm SM} : 1.05\,{\rm pb})$$

$$\sigma^{\rm NC02}_{\rm ZZ}(206.6~{\rm GeV}) = 1.23^{+0.20}_{-0.18} \pm 0.09\,{\rm pb}~~({\rm SM} : 1.07\,{\rm pb})$$

Again, the first uncertainty is statistical while the second is systematic. The SM predictions reported in parentheses have been calculated with the EXCALIBUR Monte Carlo program.

5 Anomalous Couplings

The most general parametrisation of the ZZZ and ZZγ anomalous couplings is given in Reference [1]. Assuming on-shell production of the two Z Bosons, only four couplings $f_i^{\rm V}$ $(i = 4,5); {\rm V} = \gamma, Z)$ exist, where the V superscript corresponds to an anomalous ZZV coupling. At tree level these couplings vanish in the Standard Model and a possible non-zero value would not only change the ZZ cross section, but also the shape of the distributions presented in Figure 1. Hence these distributions are fitted with a log-likelihood method, varying one anomalous f_i^V coupling at a time and fixing the other three to their Standard Model expectation [17]. The couplings are found to be compatible with their Standard Model expectation, and limits at a 95% confidence level are derived:

$$-0.48 \leq f_4^{\rm Z} \leq 0.46; \quad -0.36 \leq f_5^{\rm Z} \leq 1.03; \quad -0.28 \leq f_4^{\gamma} \leq 0.28; \quad -0.40 \leq f_5^{\gamma} \leq 0.47$$

Then, fits are performed where two couplings with one CP eigenvalue are left free, while the other two couplings with the other CP eigenvalue are fixed to their Standard Model expectation. Again, no evidence for deviations from the Standard Model is found, and the corresponding contour curves for different confidence levels can be seen in figure 3.

All these limits include results from previously published analyses at lower center-of-mass energies [2–4].

References

[1] K. Hagiwara *et al.*, Nucl. Phys. **B 282** (1987) 253.

[2] L3 Collab., M. Acciarri *et al.*, Phys. Lett. **B 450** (1999) 281.

[3] L3 Collab., M. Acciarri *et al.*, Phys. Lett. **B 465** (1999) 363.

[4] L3 Collab., M. Acciarri *et al.*, Phys. Lett. **B 497** (2001) 23.

[5] ALEPH Collab., Phys. Lett. **B 469** (1999) 287.

[6] DELPHI Collab., Phys. Lett. **B 497** (2001) 199.

[7] OPAL Collab., Phys. Lett. **B 476** (2000) 256.

[8] L3 Collab., B. Adeva *et al.*, Nucl. Inst. Meth. **A 289** (1990) 35; L3 Collab., O. Adriani *et al.*, Physics Reports **236** (1993) 1; I. C. Brock *et al.*, Nucl. Instr. and Meth. **A 381** (1996) 236; M. Chemarin *et al.*, Nucl. Inst. Meth. **A 349** (1994) 345; M. Acciarri *et al.*, Nucl. Inst. Meth. **A 351** (1994) 300; A. Adam *et al.*, Nucl. Inst. Meth. **A 383** (1996) 342; G. Basti *et al.*, Nucl. Inst. Meth. **A 374** (1996) 293.

[9] F.A. Berends, R. Kleiss and R. Pittau, Nucl. Phys. **B 424** (1994) 308; Nucl. Phys. **B 426** (1994) 344; Nucl. Phys. (Proc. Suppl.) **B 37** (1994) 163; R. Kleiss and R. Pittau, Comp. Phys. Comm. **85** (1995) 447; R. Pittau, Phys. Lett. **B 335** (1994) 490.

[10] S. Jadach, B.F.L. Ward and Z. Wąs, Preprint CERN-TH/99-235 hep-ph/9912214.

[11] S. Jadach, B.F.L. Ward and Z. Wąs, Comp. Phys. Comm **79** (1994) 503.

[12] S. Jadach *et al.*, Phys. Lett. **B 390** (1997) 298.

[13] M. Skrzypek *et al.*, Comp. Phys. Comm. **94** (1996) 216; M. Skrzypek *et al.*, Phys. Lett. **B 372** (1996) 289.

[14] R. Engel, Z Phys. **C 66** (1995) 203; R. Engel and J. Ranft, Phys. Rep. **D 54** (1996) 4244.

[15] F.A. Berends, P.H. Daverfelt and R. Kleiss, Nucl. Phys. **B 253** (1985) 441; Comp. Phys. Comm. **40** (1986) 285.

[16] The L3 detector simulation is based on GEANT Version 3.15. R. Brun *et al.*, "GEANT 3", CERN–DD/EE/84–1 (Revised), 1987. The GHEISHA program (H. Fesefeldt, RWTH Aachen Report PITHA 85/02 (1985)) is used to simulate hadronic interactions.

[17] J. Alcaraz *et al.*, Phys. Rev. **D61** (2000) 075006.

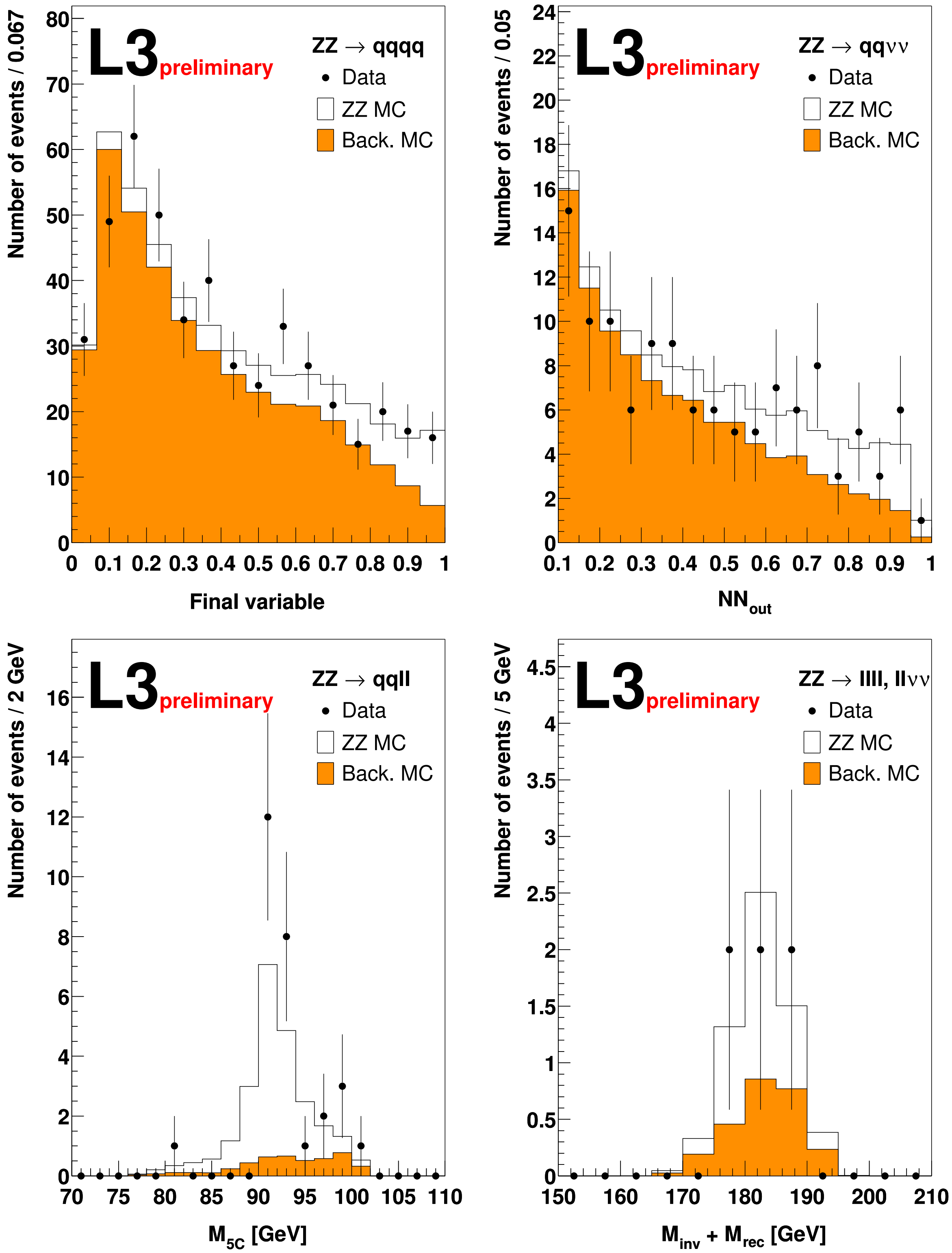

Figure 1: Distributions of the final variables of the ZZ selections for center–of–mass energies above 204 GeV: a) The final discriminant for the selected events of the $\mathrm{q\bar{q}q'\bar{q}'}$ final states, b) the neural network output NN_{out} for the selected events of the $\mathrm{q\bar{q}}\nu\bar{\nu}$ final states, c) the invariant mass M_{5C} after a constrained kinematic fit for the $\mathrm{q\bar{q}}\ell^+\ell^-$ selected events, and d) the sum of the invariant and recoil masses for the $\ell^+\ell^-\nu\bar{\nu}$ and $\ell^+\ell^-\ell'^+\ell'^-$ selected events.

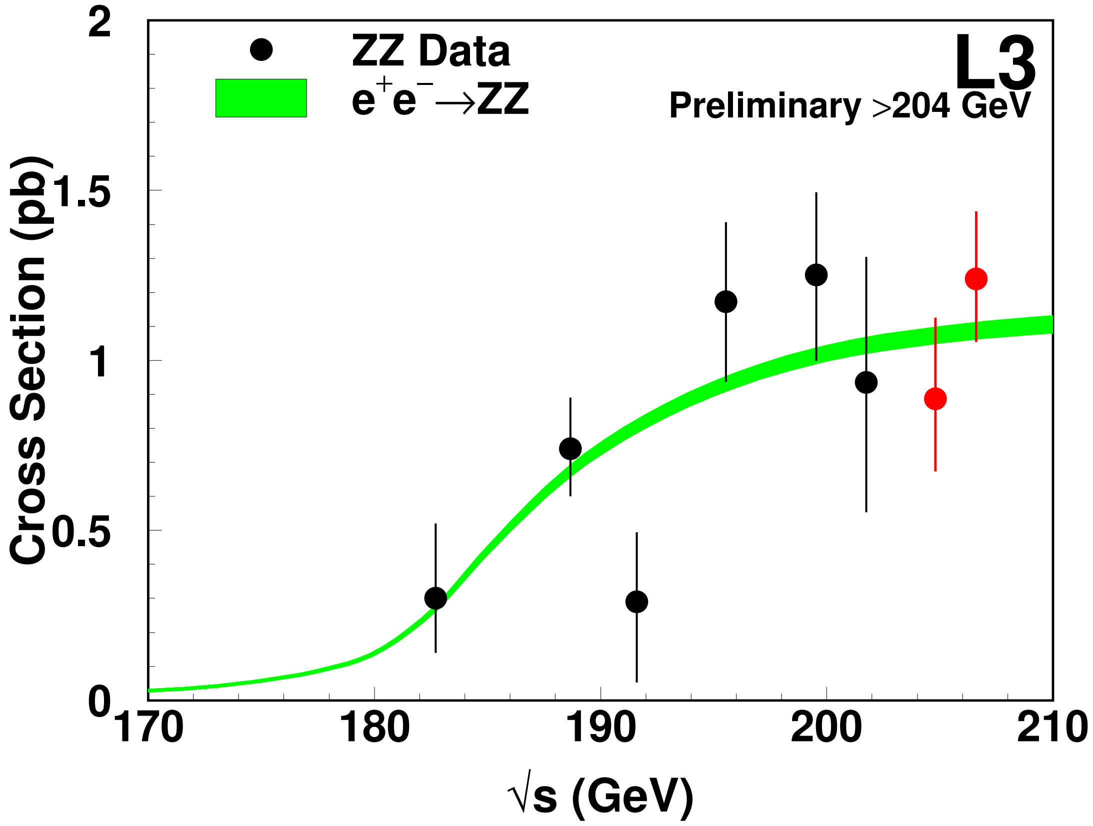

Figure 2: Standard Model prediction for the $e^+e^- \rightarrow ZZ$ cross section and the corresponding measurements. Signal definition cuts implemented with the EXCALIBUR Monte Carlo are applied and a 2% uncertainty is associated to the predictions.

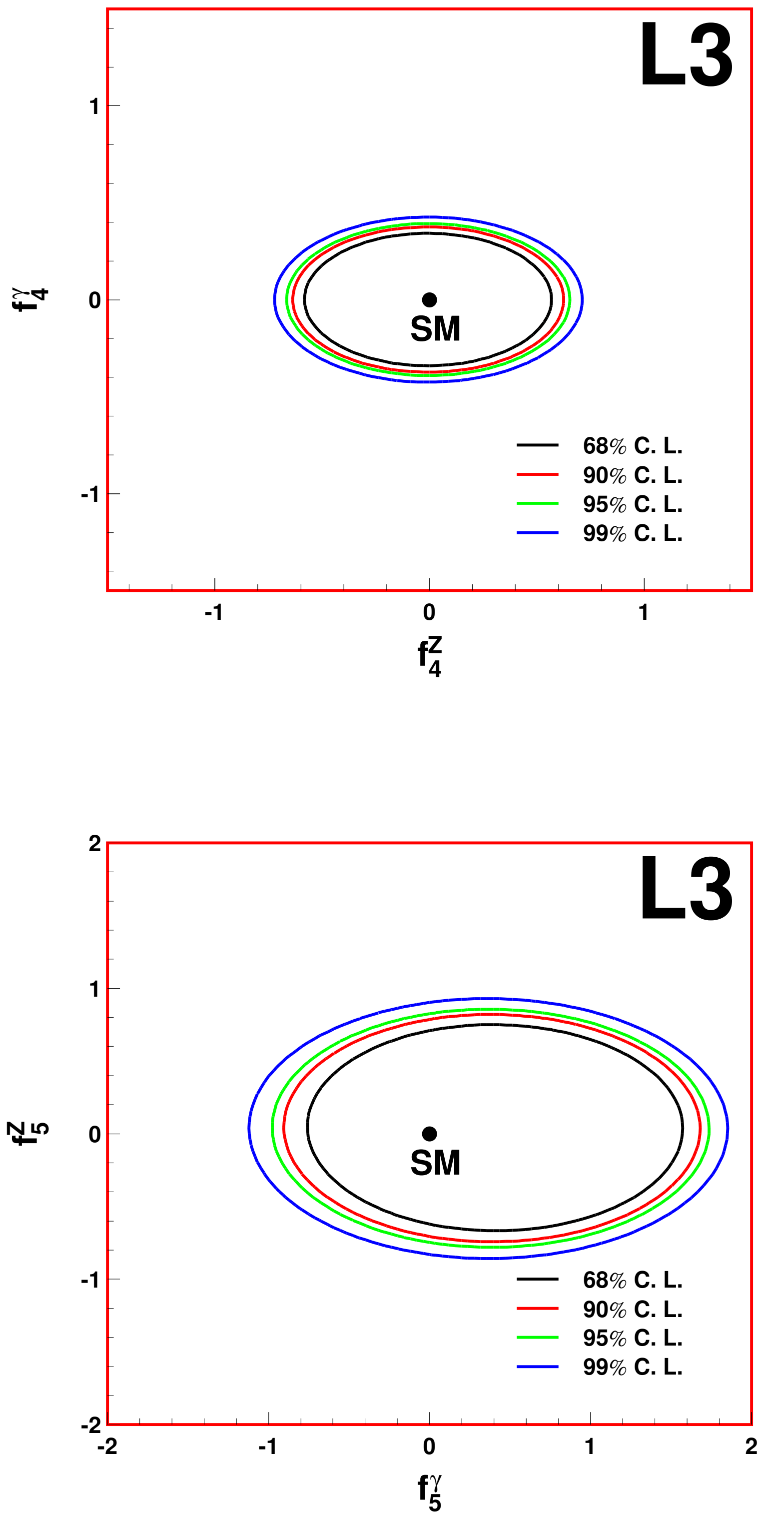

Figure 3: Two dimensional contour curves for possible anomalous couplings f_i^V of three neutral gauge bosons. For each plot, two couplings with the same CP eigenvalue have been left free in the fit, while the other two couplings are fixed to their Standard Model expectation. Contour curves for different confidence levels are shown.